



IROC Technologies
2 Square Roger Genin
Grenoble
Tel : +33.4.38.12.07.63
Fax : +33.4.38.12.96.15



ONERA
BP 74025 – 2 Avenue Edouard Belin
31055 Toulouse CEDEX 4 – France
Tel: +33.5.62.25.25.25
Fax: +33.5.62.25.25.40

AO10017

Executive Summary Report

30-May-2023

Version 1.0

Authors:

Maximilien Glorieux (IROC Technologies)
Laurent ARTOLA (ONERA)

Table of Contents

Table of Contents.....	ii
References.....	iii
1 Introduction.....	1
2 Review of Previous Work.....	2
3 Simulation of Deposited energy and SEU cross section calculation with GEANT4.....	3
4 Proposed Method to Evaluate PDI Effects.....	4
4.1 Method 1: High-Energy Degraded Beam.....	4
4.2 Method 2: Mono-Energetic Beam.....	6
5 Experimental Work.....	7
6 Analysis of the angle of incidence on the SEU occurrence.....	8
7 Experimental Results.....	9
8 Conclusion.....	10

References

- [1] ESA, "Estimation of proton induced Single Event Effect rates in very deep submicron technologies.," 2019.
- [2] N. A. Dodds, M. J. Martinez, P. E. Dodd, M. R. Shaneyfelt, F. W. Sexton, J. D. Black, D. S. Lee, S. E. Swanson, B. L. Bhuva, K. M. Warren, R. A. Reed, J. Trippe, B. D. Sierawski, R. A. Weller, N. Mahatme, N. J. Gaspard, T. Assis, R. Austin, S. L. Weeden-Wright, L. W. Massengill, G. Swift, M. Wirthlin, M. Cannon, R. Liu, L. Chen, A. T. Kelly, P. W. Marshall, M. Trinczek, E. W. Blackmore, S. .. Wen, R. Wong, B. Narasimham, J. A. Pellish and H. Puchner, "The Contribution of Low-Energy Protons to the Total On-Orbit SEU Rate," *IEEE Transactions on Nuclear Science*, vol. 62, pp. 2440-2451, 2015.
- [3] J. Guillermin, N. Sukhaseum, P. Pourrouquet, N. Chatry, F. Bezerra and R. Ecoffet, "Worst-Case Proton Contribution to the Direct Ionization SEU Rate," in *2017 17th European Conference on Radiation and Its Effects on Components and Systems (RADECS)*, 2017.
- [4] "AO8191 Error Rate Estimations inJUICE Mission Environment," 2018.

1 Introduction

The AO10017 activity consists in the evaluation of the impact of proton direct ionization (PDI) on the Single Event Effects rates of very deep sub-micron technologies in space environments [1]. The activity takes place after several other studies [2] [3] [4], which all propose different experimental and SEE rates calculation methodologies. The aim of the AO10017 activity is to build and validate a method to evaluate the SEE rates induced by proton direct ionization.

The main objectives of AO10017 activity are:

- Perform a review of the previous works performed on proton direct ionization. It includes the understanding and the comparison of the three previous methods proposed by the statement of work. In addition, the state-of-the-art review should provide a summary of all publicly available proton direct ionization experimental results.
- Perform Monte-Carlo simulations with a radiation transport code to evaluate the energy deposited in sensitive volumes representative of very deep sub-micron technologies by the direct ionization from a proton. These charge collection simulations should then be used to derive a simulated PDI cross-section and compare it with publicly available commercial results.
- Based on the learning from the state-of-the-art review, propose an experimental method to characterize the sensitivity of very deep sub-micron technologies against PDI and derive orbital error rates. This method should be reproducible and should provide coherent results independently of the technological node.
- Select a set of representative components which are expected to be sensitive to PDI, experimentally characterize their sensitivity to low energy protons and compute the PDI induced error rates, in typical space environments (LEO and GEO orbits). In addition, the selected component should be tested under heavy-ions and high-energy protons to compare the contribution of the different upset mechanisms.
- Analyze the experimental results and the error rate calculation to compare the relative contribution of PDI for the different technological nodes, space environments and shielding thicknesses.

2 Review of Previous Work

The state-of-the-art review performed in the first task of the activity identified three main approaches to experimentally characterize the PDI induced SEU sensitivity of advanced CMOS devices and derive mission error rates. Table 1 compares these three approaches.

The major interest of method [2] is that it reproduces the shielded proton spectrum of real space application at the die location. Thus, orbital error rates can be calculated very easily, by considering the acceleration factor of the beam with respect to the mission environment, without the need to convolute the measured upset cross-section with the mission proton energy spectrum. The limitation of this approach is related to the required beam characteristics, with fine tuning of the proton energy degraders.

[3] method is based on the irradiation of the component with a mono-energetic beam, at a fixed energy but with several angles of incidence. This optimizes the required beam time as the energy tuning can be time consuming. Based on these experimental results, method [3] estimates the depth and the thickness of a layer sensitive to proton direct ionization in the device. The definition of this sensitive layer is based on an arbitrary hypothesis in addition to the experimental results. Based on the definition of this layer, proton transport calculation is performed to estimate the mission proton flux which will produce upsets. [3] claims to perform irradiations at several tilt angles but assumes that the only effect of the tilt angle is the modification of the effective LET and that no other geometrical effects may alter the event sensitivity.

Finally, method [4] irradiates the device with a mono-energetic beam, at normal incidence and sweep the proton energy to characterize the upset cross-section as a function of the proton incident energy. The measured cross-section is then convoluted with the mission proton spectrum to compute the orbital error rate. The limitations of [4] are the requirements in terms of mono-energetic beam and the non-consideration of the impact of the proton incidence angle.

Table 1: Comparison of the three methods evaluate error rate induced by proton direct ionization

Criteria	[2]	[3]	[4]
Proton beam requirement	High-energy, with fine grain degrader control	Mono-energetic, at 1 low energy	Mono-energetic, at multiple low energies
Device preparation	Not needed	De-lidding and substrate thinning	De-lidding and substrate thinning
Tilt angle Consideration	Yes	No	No
Interest	Reproduction of low-energy proton flux in the test facility; Possibility to perform low and high energy proton test simultaneously	No need of energy changes for the mono-energetic, low-energy proton beam.	Accurate characterization of direct ionization cross-section peak
Limitation	Requires fine grain tuning of the beam degraders.	Several arbitrary hypotheses; focus on modelling internal layers; complex proton transport calculations	Worst case hypothesis for the proton incident angle

It is interesting to notice that [2] and [4] performed their measurements and error rate calculations on two similar 65 nm SRAM manufactured by Cypress (CY7C1512KV18 for [2] and CY7C2562XV18 for [4]). Both works reported similar error rates for orbital conditions despite their very different experimental protocols and calculation methodologies.

3 Simulation of Deposited energy and SEU cross section calculation with GEANT4

A GEANT4 application devoted to the calculation of direct ionizing deposited energy has been developed. It is based on an upgraded version of the MicroElec module that has been released in December 2020. The code has been validated thanks to comparisons with SRIM in simple cases. The cumulated and differential deposited energy distribution function have been calculated in different volumes with sizes going from 50 nm x 50 nm x 50 nm up to 500 nm x 500 nm x 300 nm silicon slab topped with various thicknesses of silicon ranging from 3 μm up to 20 μm . Deposited energy spectra have been calculated for various proton energies in the range [0.28 MeV, 10 MeV] and three angles of incidence : 0° (normal), 45° and 60°. The SEU sensitivity to direct proton ionization process has been studied as a function of the critical energy. The SEU thresholds have been chosen in the range [2 keV, 24 keV]. The SEU cross sections are plotted as a function of the incident energy. The maximum SEU cross section is observed at a typical energy that increases with the thickness of the over-layer and the angle of incidence. For large proton incident energy and quite important critical energy, the cross sections are demonstrated to increase with the angle of incidence. For flat SV (width \gg thickness), the $1/\cos(\theta)$ is validated at first order. This is not the case for SV having small lateral dimensions. For instance, cubic volumes do not follow the $1/\cos(\theta)$ law.

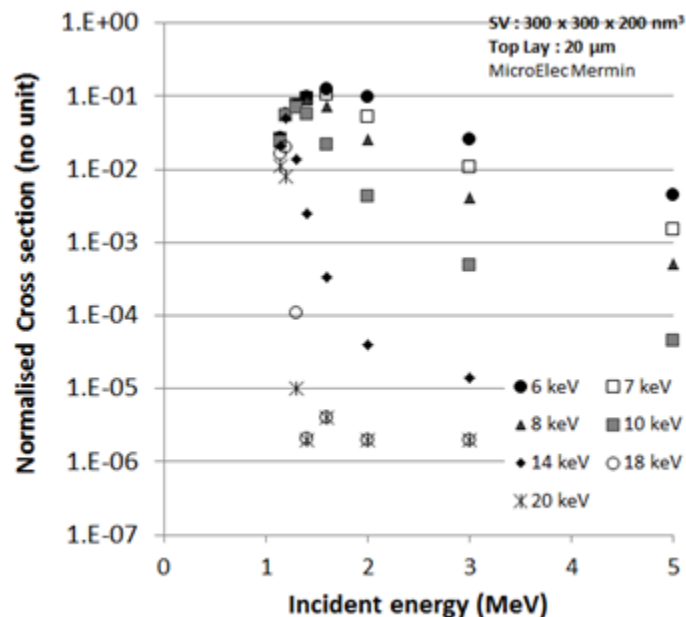


Figure 1: Normalized SEU cross section calculated for different threshold energies ranging from 6 keV up to 20 keV. These curves show a peak which becomes sharper with the increasing SEU threshold energy.

4 Proposed Method to Evaluate PDI Effects

Based on the observation from the state-of-the-art that methods [2] and [4] provides very similar results, the consortium proposed to implement in European test facilities and propose some improvements to these approaches.

These improvements are mainly related to a better consideration of the impact of the proton angle of incidence for both experimental protocols. To do so, we propose to divide the solid angle represented by a half-sphere in three regions of identical size, as shown in Figure 2. The proposed repartition is based on the assumption that protons coming from the front or the rear of the die will have equivalent effects. For tilted measurement, two roll angles must be considered to take into account the geometrical effects on the cell layout. As SRAM cell are symmetrical along X and Y axis, it is not need to perform test with four angles of incidences. The optimum angle of irradiation to het the center of each region was calculated.

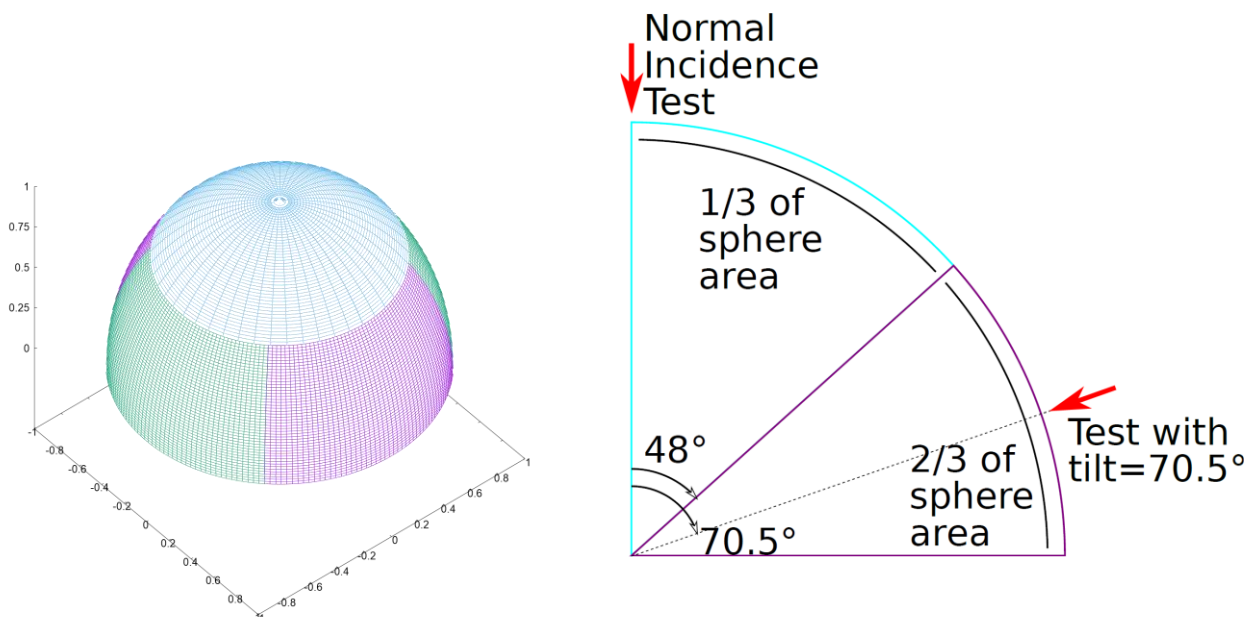


Figure 2: Half-Sphere Division in Three Region of Identical Solid Angles.

4.1 Method 1: High-Energy Degraded Beam

The objective of the first method is to reproduce the low energy proton spectrum of shielded space environment at the die level. This is achieved by degrading a high energy proton beam. The experimental protocol detailed in [2] proposed to identify the degraded beam average energy at which an SEU cross-

section peak is observed. In this configuration, the low energy proton flux at the die location is maximized and the proton energy spectrum of shielded space environment is reproduced.

A work in collaboration with RADEF facility was performed to set-up an experiment with degraded proton. The initial 55 MeV proton beam from JYU cyclotron was degraded using POM plastic degraders and aluminum sheet of different thickness (down-to 30 μm), as shown on Figure 3.

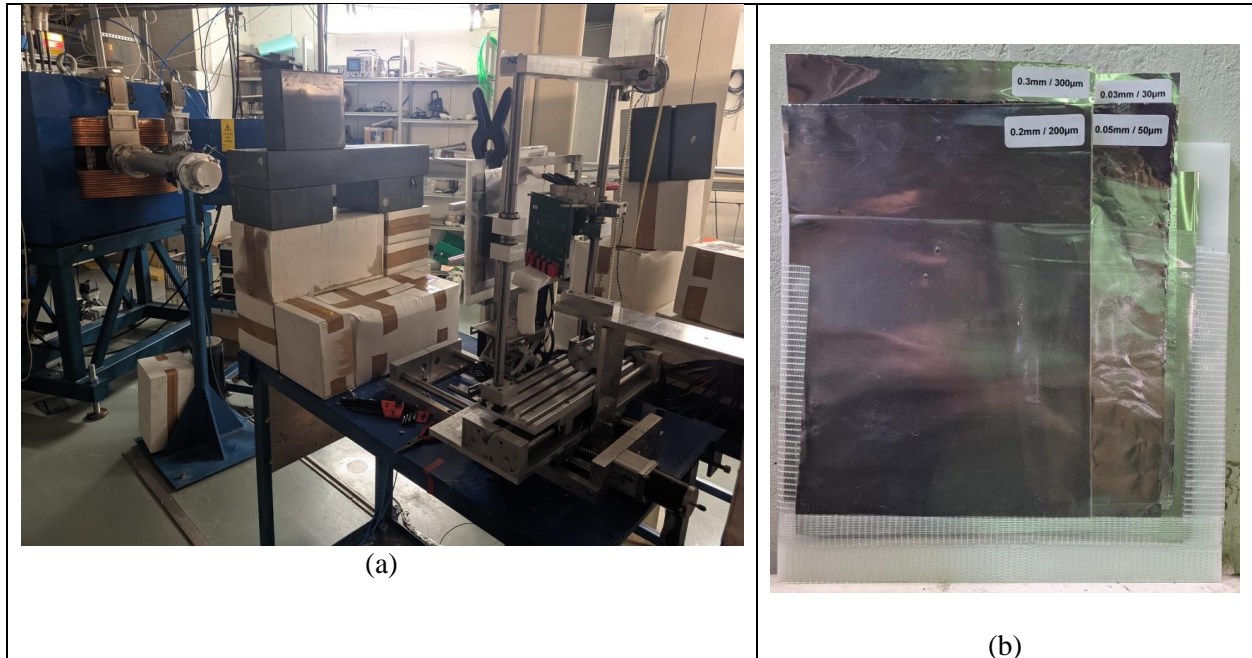


Figure 3: Degraded Beam Test Setup and Aluminum Degradation Plates with Different Thickness

The degraded beam flux and spectra was measured using a silicon detector, with an energy threshold of 1 MeV. Figure 4 compare the obtained degraded beam with the normalized proton spectra behind a shielding in LEO orbit. It shows that for energies lower than 3 MeV, at PDI effects occurs, the shape of the measured proton spectra is very similar the one in space conditions. An intensity difference can be observed and is still under investigation with RADEF.

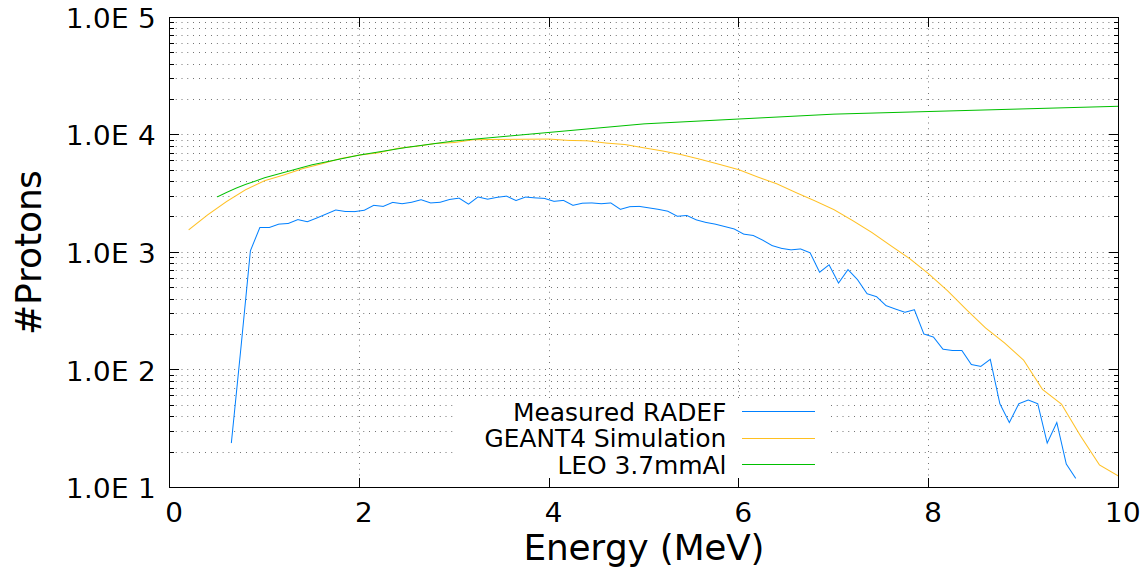


Figure 4: Comparison of Degraded Beam with LET Proton Spectra.

The experimental protocol consists in irradiating the SRAM devices in this configuration and measuring the maximum cross-section with respect to the initial 55 MeV beam. Then, the acceleration factor with respect to the orbital conditions is evaluated and used to compute the mission error rates. This measurement should be repeated for each angle of incidence.

4.2 Method 2: Mono-Energetic Beam

The objective of this methodology is to accurately characterize the PDI SEU cross-section peak in amplitude and width. The cross-section curve at this maximum will then be convoluted with the environmental proton spectra in order to compute the orbital error rate, in the same manner as this is done for high-energy protons. In order to ease this convolution process, we propose to fit the measure mono-energetic, low-energy proton cross-section to a second order polynomial function, as shown on Figure 5.

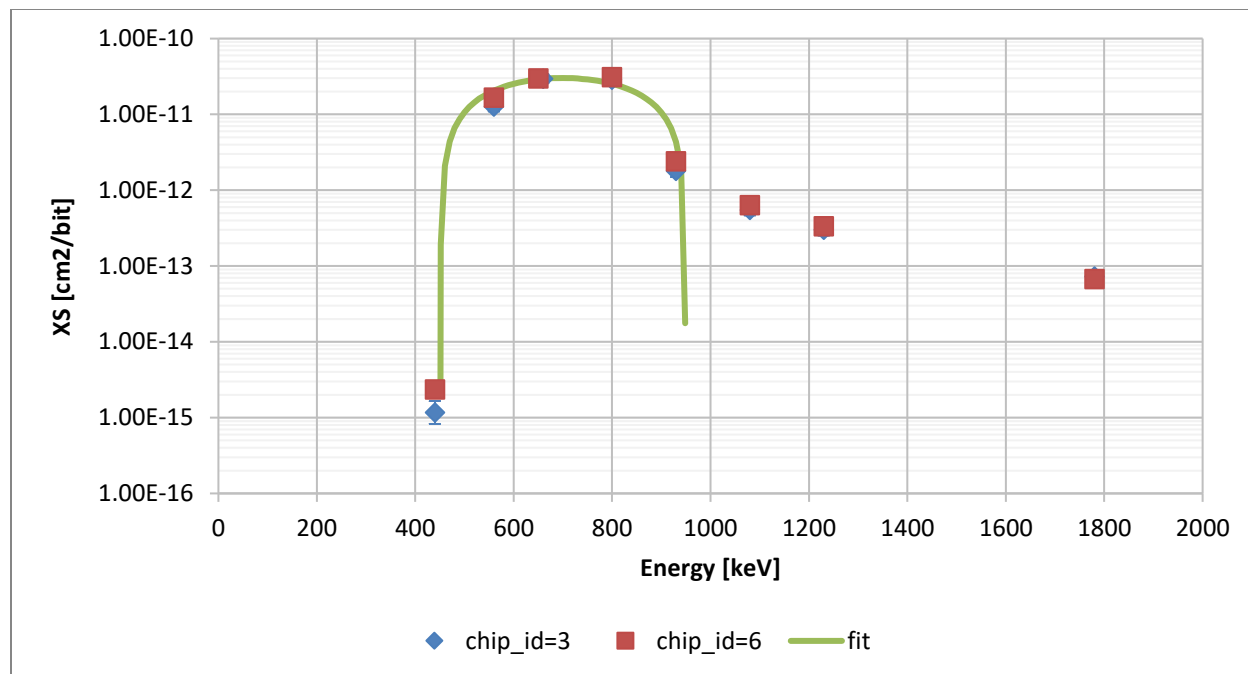


Figure 5: Mono-Energetic, Low-Energy Proton Test Results fit to 2nd Order Polynomial.

5 Experimental Work

In order to evaluate the match of both proposed methods, a set of 4 bulk SRAM devices was selected and characterized under low-energy proton, high-energy proton and heavy-ions. Table 2 lists the components that were characterized in the context of the activity. Note that the SHARC-FIN device was developed in the context of ESA activity number 4000128352/19/NL/GLC.

Table 2: List of Characterized SRAM

Manufacturer	Reference	Technological Node	Capacity
CYPRESS	CY7C2562XV18	65 nm	72 Mbit
ISSI	IS61WV204816BLL	40 nm	32 Mbit
IROC partner	28 nm SRAM	28 nm	64 Mbit
ESA/IROC	SHARC-FIN	16 nm FinFET	96 kbit

Heavy-ion test of the three planar devices were performed at UCL facility in Belgium, to take advantage of the lithium ion, whose LET is 0.35 MeV/cm²/mg. For the SHARC-FIN device, heavy-ion test was performed at RADEF Facility. Indeed, due to the FinFET technology and the lower memory capacity, higher beam flux was needed to characterize this device. High-energy proton test was performed at PSI facility in Switzerland. Degraded low-energy proton test was performed at RADEF facility while mono-energetic low-energy proton test were performed at MIRAGE, ONERA. Note that ISSI device was also tested at RADEF to compare both facilities.

6 Analysis of the angle of incidence on the SEU occurrence

Here the dependence of the roll is investigated by simulations for a 28nm technology. The simulations have been done with the ONERA simulation framework which included MUSCA SEP3 (the Monte Carlo radiation tool) and TERRIFIC (the injection faults tool) coupled with electrical simulations (with Spice simulator). The SEU cross section has been estimated with the simulation for three different proton energies, tilt and roll angles, as summarized below:

- Proton energy = 0.6MeV / 1MeV / 2 MeV ; Tilt = 0
- Proton energy = 0.6MeV / 1MeV / 2 MeV ; Tilt 60° ; Roll = 0°
- Proton energy = 0.6MeV / 1MeV / 2 MeV ; Tilt 60° ; Roll = 90°

First, the simulations results confirm the increase in the SEU cross section with the angle of the incident protons. For this 28nm Bulk technology the increase is about 40% but depend on the energy and the roll of the device. For the investigated technology, a 6 μ m of back-end-of-line (BEOL) has been used. The thickness of the BEOL must change the range of the protons in the device, especially as a function of the tilt of the protons. Here at 0.6MeV, most the proton energy is deposited in the BEOL and the remaining energy is not enough to induce an upset in the SRAM bit. However, it is important to note that the SEU cross section is also dependent to the roll of the device. Figure 6 shows that for low energy protons which crosses the N-well and P-well of the SRAM, the SEU cross section is lower (Oy). This observation is in total adaptation with the experimental data measured during the low energy proton irradiation campaigns. It is important to note that, no multiple bit upset has been observed during all the simulations, whatever the tilt and the roll and the energy (below 2MeV) of the incident protons.

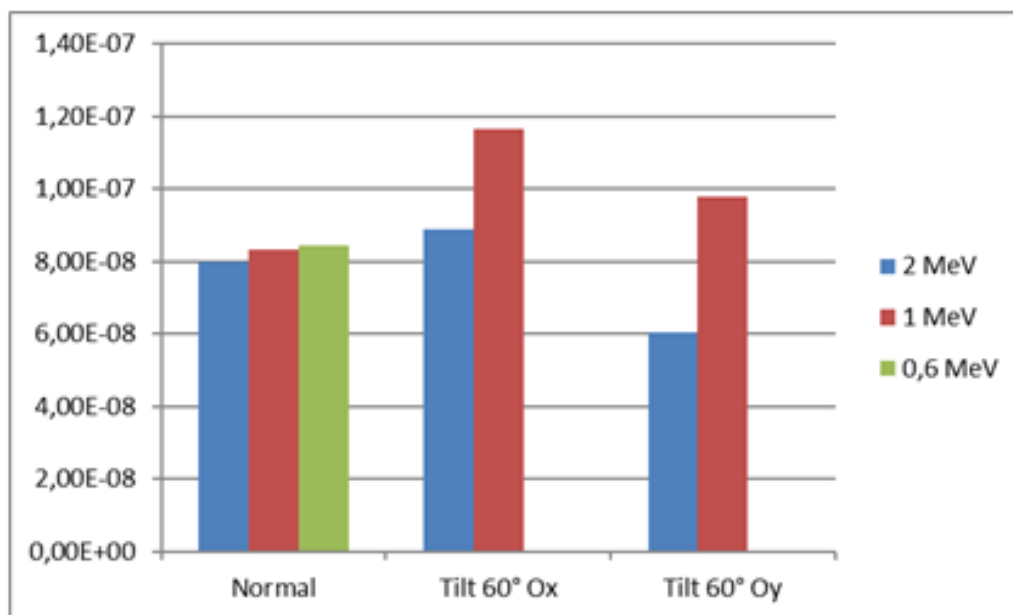


Figure 6: Simulated SEU cross section (in μ m) of 28nm SRAM LP process as a function of angle configuration and for three energy: 0.6V (green), 1MeV (red), 2MeV (blue).

Figure 7 (b) demonstrates the electrical feedback loop operated by the INV2 (in red) which maintains the stored state of the SRAM cell. The electrical feedback loop is stronger for the low energy protons crossing the N-well and P-well because the two inverters are disturbed. On the other hand, as shown in Figure 7(a) for the incident protons crossing only one of the two inverters the collected charges pull the two inverters to charge their stored state. The analysis identifies the origin of the roll dependence of the SEU cross section induced by low energy protons at the ionizing peak.

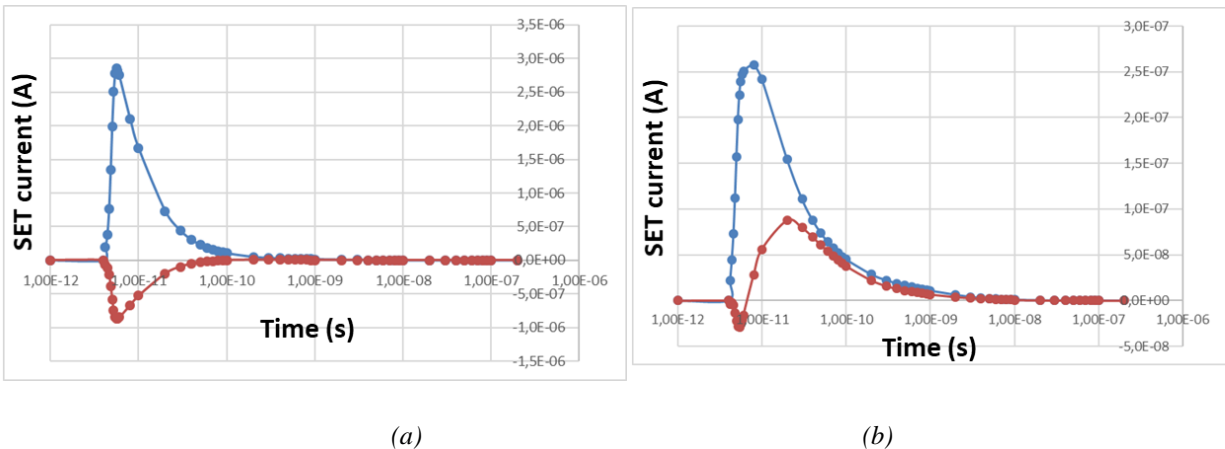


Figure 7: SET transient response of inverter 1 (in blue) and inverter 2 (in red) induced by a 1MeV protons striking the SRAM cell: (a) along the access gate (Ox) of the 6T SRAM cells, (b) across the N-well and P-well (Oy) of the 6T SRAM cells

7 Experimental Results

Following to the different test campaigns, the experimental results were analyzed for all devices and the orbital error rates for typical LEO mission in quiet was assessed. Figure 8 reports the contribution of each type of radiation to the mission error rates, for each angle of incidence and tested device. The following observation can be made:

- Both methods to evaluate the contribution of proton direct ionization provides very similar results, for all considered device and angle of incidence, with relative difference lower than 2X.
- The overall error rates are dominated by indirect proton ionization for all tested components and angle of incidence. Note that this is not the case in worst case conditions, due to the higher magnitude of low energies protons in solar flares (compared to trapped particles).
- The devices with the highest sensitivity to proton direct ionization are the ISSI and 28 nm devices.
- For all tested devices, a strong decrease of the PDI sensitivity in roll=0 was observed compared to the normal incidence and the roll=90 angle of incidence. Note that this observation could not be confirmed on the SHARC-FIN device due to beam time limitation but similar trends was identified with low LET heavy-ions.

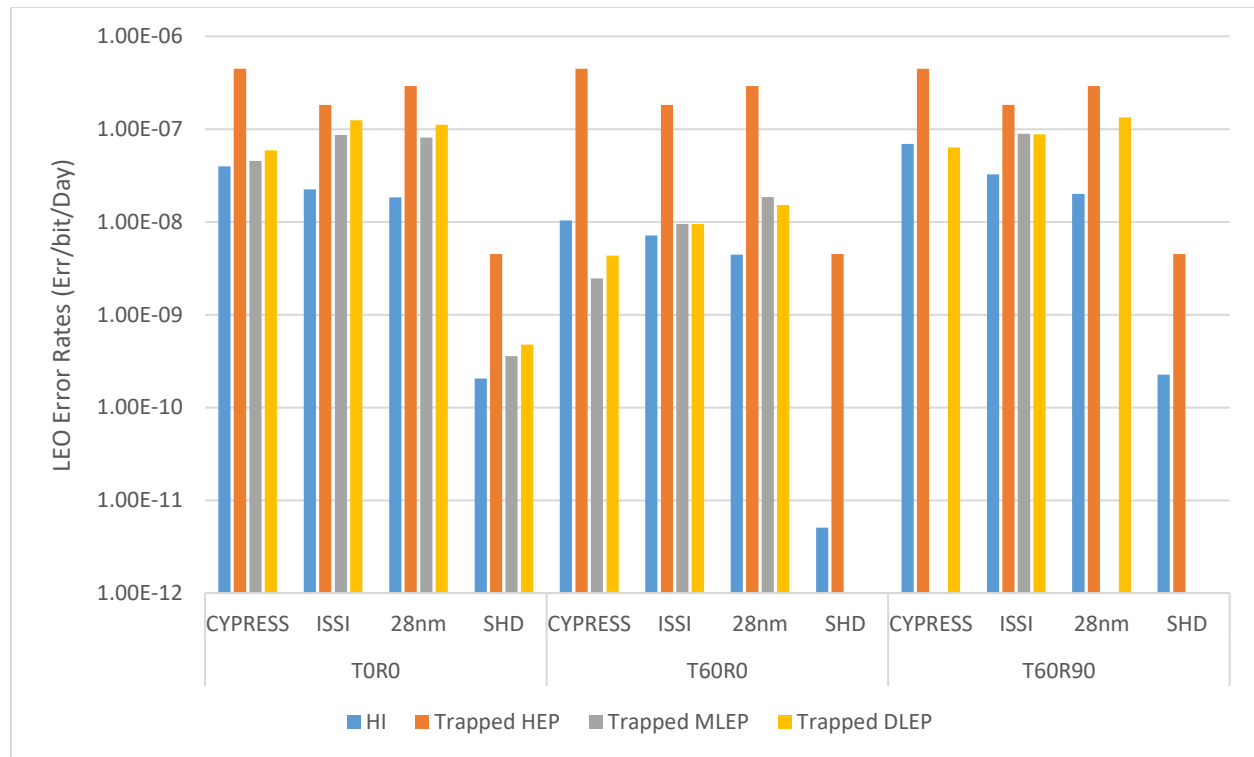


Figure 8: Error Rate for LEO Orbit in Quiet Conditions

8 Conclusion

Following the state-of-the-art review, two methodologies to evaluate the contribution of proton direct ionization to the orbital SEU error rates were proposed. Both approaches were successfully applied on a set of 4 bulk SRAM devices, manufactured in advanced process nodes from 65 nm down-to 16 nm FinFET. For these 4 devices, both experimental protocols provided comparable results in term of orbital error rates and the two methods can be considered as equivalent for bulk SRAM devices, letting the possibility to select one of them depending of experimental constraints (device package, sensitivity, beam time availability...).

The degraded beam methodology is well suited for devices of large capacity, which do not require high flux to get statistically significant number of events. In such conditions, this approach is probably more efficient than the mono-energetic beam as it is not needed to de-lid the devices and the beam degrader configuration can be adjusted quickly.

For devices which are less sensitive, the mono-energetic methodology is recommended because it provides a better identification of the device sensitivity. In addition, the degraded beam test require high flux and fluence, leading to an important activation of the degrader materials.